CHEMISTRY
A EUROPEAN JOURNAL

FULL PAPER

DOI: 10.1002/chem.201202457

Chiral Benzamidinate Ligands in Rare-Earth-Metal Coordination Chemistry

Paul Benndorf, Jochen Kratsch, Larissa Hartenstein, Corinna M. Preuss, and Peter W. Roesky*[a]

Abstract: The treatment of the recently reported potassium salt (*S*)-*N*,*N*′-bis-(1-phenylethyl)benzamidinate ((*S*)-KPEBA) and its racemic isomer (*rac*-KPEBA) with anhydrous lanthanide trichlorides (Ln = Sm, Er, Yb, Lu) afforded mostly chiral complexes. The tris(amidinate) complex [{(*S*)-PEBA}$_3$Sm], bis(amidinate) complexes [{Ln(PEBA)$_2$(μ-Cl)}$_2$] (Ln = Sm, Er, Yb, Lu), and mono(amidinate) compounds [Ln(PEBA)(Cl)$_2$(thf)$_n$] (Ln = Sm, Yb, Lu) were isolated and structurally characterized. As a result of steric effects, the homoleptic 3:1 complexes of the smaller lanthanide atoms Yb and Lu were not accessible. Furthermore, chiral bis(amidinate)–amido complexes [{(*S*)-PEBA}$_2$Ln{N(SiMe$_3$)$_2$}] (Ln = Y, Lu) were synthesized by an amine-elimination reaction and salt metathesis. All of these chiral bis- and tris(amidinate) complexes had additional axial chirality and they all crystallized as diastereomerically pure compounds. By using *rac*-PEBA as a ligand, an achiral *meso* arrangement of the ligands was observed. The catalytic activities and enantioselectivities of [{(*S*)-PEBA}$_2$Ln{N(SiMe$_3$)$_2$}] (Ln = Y, Lu) were investigated in hydroamination/cyclization reactions. A clear dependence of the rate of reaction and enantioselectivity on the ionic radius was observed, which showed higher reaction rates but poorer enantioselectivities for the yttrium compound.

Keywords: amidinate · hydroamination · lanthanides · ligand effects · rare-earth metals

Introduction

Amidinates and their closely related guanidinates are a well-established class of N-chelating ligands that form complexes with almost all metals in the periodic table.[1] In general, amidinates are monoanionic nitrogen-donor ligands of the formula [RC(NR′)$_2$]$^-$. Because substituents R and R′ can be easily varied in numerous ways, the steric and electronic properties of these ligands can be effectively tuned. Beside their ease of accessibility, this high flexibility in ligand design is one factor that makes amidinates very popular as ligands in coordination chemistry. The versatility of amidinates as ligands is also reflected in the chemistry of the rare-earth elements. The rare-earth-metal chemistry of amidinate was pioneered by Edelmann and co-workers about two decades ago.[2] Since then, the number of publications in this area has been rapidly expanding.[2b,3] The most intensely studied amidinate ligand, *N*,*N*′-bis-(trimethylsilyl)-benzamidinate,[4] has been found to stabilize lanthanide complexes in all three of its accessible oxidation states (+II, +III, +IV).[2b] This ligand can also be used to synthesize mono-, bis-, and tris(amidinate) complexes. Moreover, numerous catalytic applications of lanthanide–amidinate complexes, such as the polymerization of ethene[5] and isoprene,[6] hydroboration,[7] hydrosilylation,[8] and intramolecular hydroamination/cyclization reactions,[9] have been reported.[2b,3b,10]

Surprisingly, relatively few chiral amidines are known in coordination chemistry (Scheme 1) and only complexes of Group 4 metals,[11] molybdenum,[12] nickel,[12,13] and rhodium,[14] but no lanthanide complexes had been presented in the literature before we entered this field.[15]

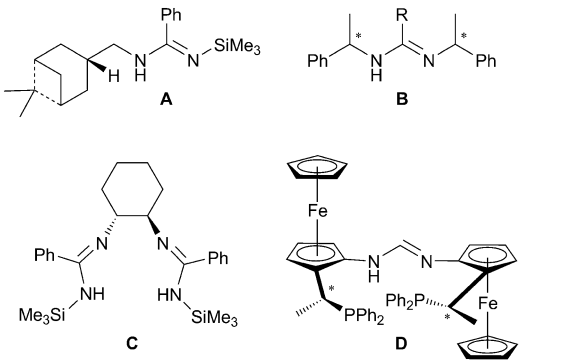

Scheme 1. Known chiral amidinates that are used as ligands in coordination chemistry.

Recently, we reported an improved synthesis of the chiral amidine *N*,*N*′-bis-(1-phenylethyl)benzamidine (HPEBA) and its corresponding lithium- and potassium salts (LiPEBA and KPEBA, respectively).[15a] KPEBA was synthesized by the treatment of KH with HPEBA in boiling THF (Scheme 2).

[a] Dr. P. Benndorf, Dipl.-Chem. J. Kratsch, L. Hartenstein, Dipl.-Chem. C. M. Preuss, Prof. Dr. P. W. Roesky
Institut für Anorganische Chemie
Karlsruher Institut für Technologie (KIT)
Engesserstrasse 15, 76131 Karlsruhe (Germany)
Fax: (+49) 721-608-44854
E-mail: roesky@kit.edu

Supporting information for this article is available on the WWW under http://dx.doi.org/10.1002/chem.201202457.

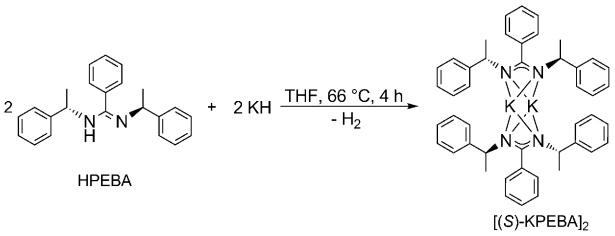

Scheme 2. Synthesis of (*S*)-KPEBA from KH and (*S*)-HPEBA.[15a]

HPEBA was first reported about 30 years ago by Brunner et al.[12,14b] By using this chiral ligand, we communicated the first chiral rare-earth–amidinate complexes and determined their catalytic activities and enantioselectivities in hydroamination reactions.[15b,16] Based on these results, herein, we report a full account of the reactivity of the PEBA ligand in its coordination chemistry of rare-earth elements, including structural investigations. Also, the influence of the ionic radius of different lanthanide metals onto the coordination of the PEBA ligand is reported. Moreover, the application of some selected compounds as catalysts in the enantioselective intramolecular hydroamination reactions of non-activated terminal amino olefins is shown. In our investigation, we focused on the enantiopure version of the PEBA ligand, but, in some cases, its racemic form was also used because it tended to crystallize more easily. Moreover, the enantiopure and racemic forms had an influence on the chirality of the metal center. By using both forms, a comparison was possible.

Results and Discussion

In a systematic approach, we synthesized mono-, di-, and trisubstituted amidinate complexes of the rare-earth elements.[16]

Mono- and bis(amidinate)–chloro complexes: The mono(amidinate)–dichloro complexes of $[Ln(PEBA)(Cl)_2(thf)_n]$ (Ln = Sm (**1**) , $n=3$; Ln = Yb (**2**), Lu (**3**), $n=2$) were obtained by the reactions of anhydrous lanthanide trichlorides with (*S*)- (Ln = Yb, Lu) and *rac*-KPEBA (Ln = Sm) in THF at room temperature (Scheme 3). In the case of samarium, the ligand had to be added dropwise to the suspension of $SmCl_3$ to avoid the formation of higher substituted species. This observation was due to the larger ionic radius of samarium compared to ytterbium and lutetium.[17] Complexes with the larger lanthanides, lanthanum and cerium, could not be obtained by using our synthetic approach.

Single crystals of compounds **1**, **2**, and **3** were obtained by the slow diffusion of *n*-pentane into a solution of the complexes in THF. Single crystals of the samarium compounds were only obtained for the achiral complex, which was synthesized by using *rac*-KPEBA. The enantiomerically pure analogue could also be obtained in situ (see below) but single crystals could not be grown. The racemic form of compound **1** crystallizes in the space group $P2_1/c$ with four

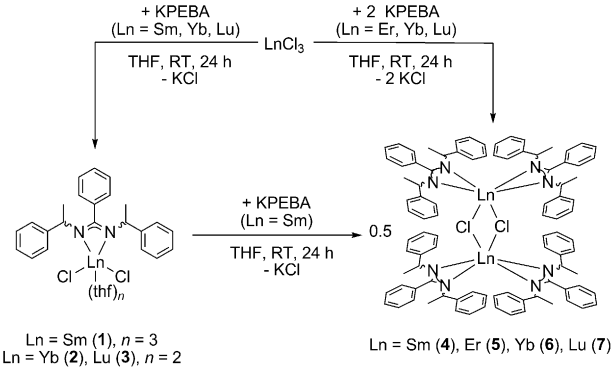

Scheme 3. Synthesis of mono- and bis(amidinate)–chloro complexes.

molecules in the unit cell (Figure 1). The samarium atom is sevenfold coordinated by the PEBA ligand, two chloride atoms, and three molecules of THF in a distorted pentagonal-bipyramidal fashion. The N1-C1-N2 angle (114.4(2)°)

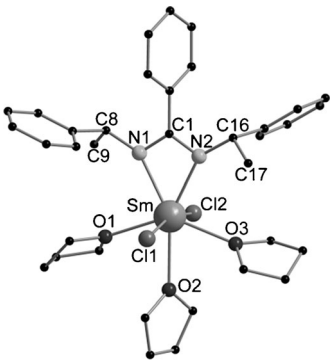

Figure 1. Solid-state structure of complex **1**; hydrogen atoms are omitted for clarity. Selected bond lengths [Å] and angles [°]: C1–N1 1.334(4), C1–N2 1.337(3), C1–C2 1.510(4), C1–Sm 2.887(3), C8–N1 1.466(3), C8–C9 1.517(4), C8–C10 1.527(4), C16–N2 1.468(3), C16–C17 1.516(4), C16–C18 1.528(4), N1–Sm 2.437(2), N2–Sm 2.440(2), O1–Sm 2.486(2), O2–Sm 2.580(2), O3–Sm 2.512(2), Cl1–Sm 2.6705(8), Cl2–Sm 2.6685(8); N1-C1-N2 114.4(2), N1-C1-C2 123.1(2), N2-C1-C2 122.5(2), N1-C1-Sm 57.17(14), N2-C1-Sm 57.30(14), N1-C8-C9 109.9(2), N1-C8-C10 112.4(2), C9-C8-C10 112.6(3), N2-C16-C17 109.5(2), N2-C16-C18 112.3(2), C17-C16-C18 112.5(2), C1-N1-C8 118.6(2), C1-N1-Sm 95.4(2), C8-N1-Sm 145.7(2), C1-N2-C16 118.5(2), C1-N2-Sm 95.2(2), C16-N2-Sm 146.3(2), N1-Sm-N2 54.84(8), N1-Sm-O1 81.62(8), N2-Sm-O1 136.17(7), N1-Sm-O3 137.72(7), N2-Sm-O3 83.39(7), O1-Sm-O3 140.43(7), N1-Sm-O2 151.39(7), N2-Sm-O2 153.76(7), O1-Sm-O2 69.86(7), O3-Sm-O2 70.62(7), N1-Sm-Cl2 93.33(5), N2-Sm-Cl2 98.39(5), O1-Sm-Cl2 87.93(4), O3-Sm-Cl2 85.91(4), O2-Sm-Cl2 83.65(4), N1-Sm-Cl1 99.60(5), N2-Sm-Cl1 94.42(5), O1-Sm-Cl1 87.50(4), O3-Sm-Cl1 88.87(4), O2-Sm-Cl1 81.87(4), Cl2-Sm-Cl1 165.51(2).

and the C1–N distances (C1–N1 1.334(4) Å, C1–N2 1.337(3) Å) are in the expected range.[15b]

In the ^{1}H NMR spectrum of compound **1**, very broad signals were observed owing to the paramagnetism of the samarium atom, which resulted in a non-characteristic spectrum.

Isostructural compounds **2** and **3** crystallize in the chiral space group *C*2 with two molecules in the unit cell

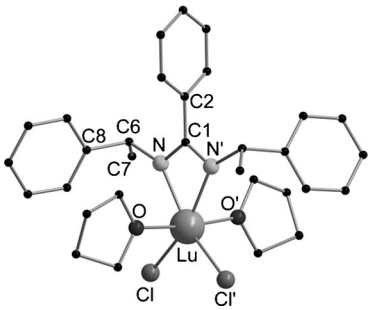

Figure 2. Solid-state structure of compound **3**; hydrogen atoms are omitted for clarity. Selected bond lengths [Å] and angles [°] (data for the isostructural compound **2** are also given): **3**: C1−N 1.334(4), C1−Lu 2.743(4), C6−N 1.474(5), C6−C8 1.519(5), C6−C7 1.525(5), N−Lu 2.303(3), O−Lu 2.281(2), Cl−Lu 2.5341(10); N-C1-N 113.8(4), N-C1-C2 123.1(2), N-C1-Lu 56.9(2), C2-C1-Lu 180.0 (1), C8-C6-C7 111.8(3), N-C6-C7 109.3(3), N-C6-C8 110.0(3), C1-N-Lu 94.1(2), O-Lu-N 88.8(2), O-Lu-N 85.8(2), O-Lu-Cl 87.9(12), O-Lu-Cl 96.05(12), Cl-Lu-Cl 101.17(6), N-Lu-N 58.0 (2); **2**: C1−N 1.343(5), C1−C2 1.496(7), C1−Yb 2.754(5), C6−N 1.478(5), C6−C8 1.522(6), C6−C7 1.531(6), N−Yb 2.300(4), O−Yb 2.293(3), Cl−Yb 2.5441(14); N-C1-N 112.7(5), N-C1-C2 123.7(2), N-C1-Yb 56.3(2), N-C6-C8 111.0(3), N-C6-C7 108.9(4), C8-C6-C7 112.0(4), C1-N-C6 120.6(3), C1-N-Yb 94.6(3), C6-N-Yb 144.6(3), O-Yb-O 172.4(3), O-Yb-N 88.2(2), N-Yb-N 58.2(2), Cl-Yb-Cl 100.83(8).

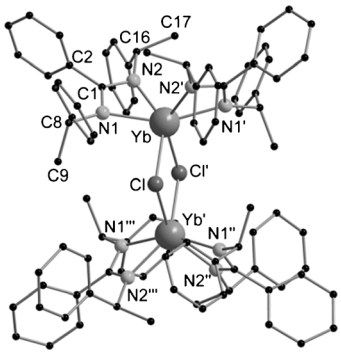

Figure 3. Solid-state structure of compound **6**; hydrogen atoms are omitted for clarity. Selected bond lengths [Å] and angles [°] (data for isostructural compounds **4** and **7** are also given): **6**: C1−N1 1.330(6), C1−N2 1.328(5), C1−C2 1.501(4), C1−Yb 2.729(3), C8−N1 1.480(4), C8−C9 1.536(6), C16−N2 1.472(5), C16−C17 1.528(7), N1−Yb 2.342(3), N2−Yb 2.273(3), Cl−Yb 2.6724(7), Yb−Yb 4.2046(6); N1-C1-N2 115.1(3), N1-C1-C2 120.8(4), N2-C1-C2 124.1(4), N1-C1-Yb 59.0(2), N2-C1-Yb 56.1(2), C2-C1-Yb 176.4(3), N1-C8-C9 110.1(3), N2-C16-C17 108.8(3), C1-N1-C8 119.5(3), C1-N1-Yb 91.8(2), C8-N1-Yb 148.7(2), C1-N2-C16 120.2(3), C1-N2-Yb 95.0(2), C16-N2-Yb 144.7(3), Yb-Cl-Yb 103.75(3), N2-Yb-N1 58.13(11), Cl-Yb-Cl 76.25(3); **4**: C1−N1 1.331(6), C1−N2 1.341(5), C1−C2 1.499(5), C1−Sm 2.831(3), C16−N2 1.478(5), C16−C17 1.527(6), C8−N1 1.477(4), C8−C9 1.527(6), N2−Sm 2.341(3), N1−Sm 2.441(3), Cl−Sm 2.7682(7); N1-C1-N2 114.7(3), N1-C1-C2 124.3(4), N2-C1-C2 121.1(4), N2-Sm-N1 56.06(11), Sm-Cl-Sm 103.74(3), Cl-Sm-Cl 76.26(3); **7**: C1−N1 1.325(5), C1−N2 1.345(5), C1−C2 1.507(4), C1−Lu 2.725(3), C16−N2 1.483(4), C8−C9 1.547(5), C16−C17 1.521(6), C8−N1 1.482(4), N1−Lu 2.343(2), N2−Lu 2.256(3), Cl−Lu 2.6648(6); N1-C1-N2 114.8(3) N1-C1-C2 124.4(4), N2-C1-C2 120.8(4), N2-Lu-N1 58.51(9), Lu-Cl-Lu 103.81(3), Cl-Lu-Cl 76.19(3).

(Figure 2). In each case, the central metal atom is coordinated by one PEBA ligand, two chloride atoms, and two THF molecules in a distorted octahedral fashion. The two chloride atoms are coordinated in a *cis* arrangement (Cl-Yb-Cl′ 100.83(8), Cl-Lu-Cl′ 101.17(6)) and are also coplanar to the NCN plane. A crystallographic *C*2 axis through the phenyl group at the central carbon atom of the PEBA ligand and the lanthanide ion is observed. Thus, only half of the molecule is located in the asymmetric unit. The distances between the lanthanide center and the chloride atoms are 2.544(1) Å (**2**) and 2.5341(10) Å (**3**), the Ln−N bond length is 2.300(4) Å in complex **2** and 2.303(3) Å in complex **3**. The N-C1-N′ angles are 112.7(5)° (**2**) and 113.8(4)° (**3**) and the N-Ln-N′ angles are 58.2(2)° (**2**) and 58.0(2)° (**3**).

The bis(amidinate)–chloro–lanthanide complexes [{Ln(PEBA)$_2$(μ-Cl)}$_2$] (Sm (**4**), Er (**5**), Yb (**6**), Lu (**7**)) were synthesized by a salt-metathesis reaction from $LnCl_3$ and two equivalents of either (*S*)- (Yb, Lu) or *rac*-KPEBA (Er). Compounds **6** and **7** were best accessed in a one-pot synthesis. The formation of their corresponding tris(amidinate) complexes was prevented owing to steric reasons and, thus, clean conversion into the bis complexes was observed. The synthesis of compound **5** was less straightforward. The desired compound could only be isolated in 10% yield. The bis-
(amidinate) complex of the larger samarium cation could not be obtained in a one-step reaction. To obtain compound **4**, chiral mono(amidinate) complex **1** first had to be synthesized in situ and then the second equivalent of KPEBA had to be added dropwise into this solution. All of these complexes have been characterized by standard analytical/spectroscopic techniques. In the NMR spectra of diamagnetic compound **3**, some additional signals were always observed. We suggest that these signals are the result of a ligand-redistribution reaction.

In the solid state, compounds **4**, **5**, **6**, and **7** form dimers that are bridged by two chlorine atoms (Figure 3). The observed arrangement is similar to that of the comparable guanidinate complex, [({[(Me$_3$Si)$_2$NC(N*i*Pr)$_2$]}$_2$SmCl)$_2$], which is also dimeric in the solid state.[18] Compounds **4**, **6**, and **7** are isostructural and crystallize in the cubic space group *I*23 with six molecules in the unit cell. The asymmetric unit only consists of a quarter of a molecule. Thus, two crystallographic *C*2 axes are observed in compounds **4**, **6**, and **7**; one *C*2 axis is seen along the Cl−Cl′ bond whereas the other one is observed along the Ln−Ln′ bond. Helical chirality is formed along this axis. Only the helical Λ enantiomer[19] is observed, thus showing that one diastereomer is exclusively formed in the solid state. The lanthanide atoms are coordinated by four nitrogen atoms of two ligands and two chloride anions. The PEBA ligands of the same lanthanide atom are arranged in an eclipsed fashion to each other and in a staggered orientated to the chlorine atoms. The ligand itself binds asymmetrically to the lanthanide atoms; the Ln−N bond lengths differ by 0.06–0.10 Å (Sm−N1 2.441(3) Å, Sm−N2 2.341(3) Å, Yb−N1 2.342(3) Å, Yb−N2 2.273(3) Å, Lu−N1 2.343(2) Å, Lu−N2 2.256(3) Å). We suggest that this asymmetry is caused by steric repulsion between the ligands. The N1−Cl distances (3.597 Å (**4**), 3.443 Å (**6**), 3.432 Å (**7**)) are smaller than the N2−Cl distances (3.996 Å (**4**), 3.864 Å

(**6**), 3.849 Å (**7**)), which leads to larger repulsion between the N1 and Cl atoms. The N1–C1 and N2–C1 distances are almost equal and the N1-C1-N2 angles are similar to those reported for the mono(amidinate) compounds (114.7(3)° (**4**), 115.1(3)° (**6**), 114.8(3)° (**7**)).

Complex **5**, which was synthesized by using *rac*-KPEBA, crystallizes in the centrosymmetric space group $P\bar{1}$ with two molecules of the complex and one molecule of *n*-pentane in the unit cell. In contrast to *rac*-KPEBA and compound **1**, the crystal does not contain both enantiomers, but instead, compound **5** crystallizes in an achiral *meso* arrangement. As a result, a different orientation of the ligands is observed in comparison to the chiral complexes, thus resulting in significant changes in the bonding parameters. The chloro ligands are now coordinated *gauche* to the PEBA ligands. The Cl-Er-Cl angle (80.43(5)–80.54(5)°) is much larger than in the chiral complexes (76.2° in all cases), and the two amidinate ligands are coordinated almost symmetrically to the lanthanide atoms (Er–N1 2.322(5) Å, Er–N2 2.314(6) Å, Er–N3 2.345(5) Å, Er–N4 2.314(5) Å). The N-C-N angles are (113.8(5)–114.9(6)°) in the same region as in compounds **4**, **6**, and **7**.

All of the complexes were fully characterized by analytical spectroscopic techniques. The NMR spectra of diamagnetic compound **7** showed characteristic sets of signals. Only one signal was observed for each of the methine (^{1}H NMR: $\delta = 4.15$ ppm; ^{13}C{^{1}H} NMR: $\delta = 58.3$ ppm) and methyl groups (^{1}H NMR: $\delta = 1.44$ ppm; ^{13}C{^{1}H} NMR: $\delta = 21.7$ ppm) in the ^{1}H and ^{13}C{^{1}H} NMR spectra of compound **7**, thus indicating that the ligands bind symmetrically to the lanthanide atoms in solution. The chemical shifts of these signals were in the range of those in KPEBA (methyl group: ^{1}H NMR: $\delta = 1.30$ ppm, ^{13}C{^{1}H} NMR: $\delta = 22.3$ ppm; methine group: ^{1}H NMR: $\delta = 4.22$ ppm, ^{13}C{^{1}H} NMR: $\delta = 57.2$ ppm).[15a]

Paramagnetic compound **4** shows two sets of signals in its NMR spectra. In the ^{1}H NMR spectrum, a quartet at $\delta = 4.16$ ppm (^{13}C{^{1}H} NMR: $\delta = 49.9$ ppm) and a multiplet at $\delta = 5.32$ ppm (^{13}C{^{1}H} NMR: $\delta = 57.8$ ppm) are observed for the methine group. The methyl groups generate two doublets in the ^{1}H NMR spectrum at $\delta = 1.50$ and 1.23 ppm (^{13}C{^{1}H} NMR: $\delta = 26.5$ and 22.1 ppm), respectively. In the ^{1}H NMR spectrum, the signals for the aromatic protons appear as multiplets between $\delta = 7.63$–5.79 ppm. As result of the paramagnetism, two protons could not be assigned and, in the ^{13}C{^{1}H} NMR spectrum, the signals for the quaternary carbon atoms were not observed.

Tris(amidinate) complexes: The homoleptic samarium tris(amidinate) complex [{(*S*)-PEBA}$_3$Sm] (**8**) was synthesized by amine-elimination from [Sm{N(SiHMe$_2$)$_2$}$_3$(thf)$_2$] and (*S*)-HPEBA at room temperature in THF (Scheme 4).

Single crystals were obtained from a hot solution in THF. Compound **8** crystallizes in the cubic space group $P2_13$ with four molecules of compound **8** (Figure 4) and four molecules of heavily disordered THF in the unit cell. The solvent molecules were suppressed by using the SQUEEZE routine in

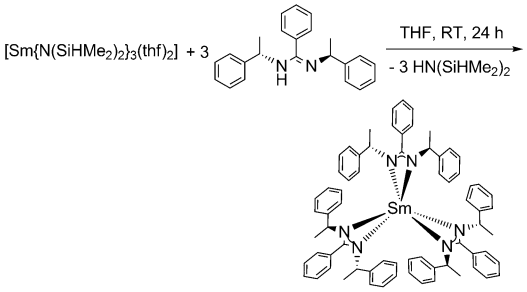

Scheme 4. Synthesis of the tris(amidinate) complex **8.**

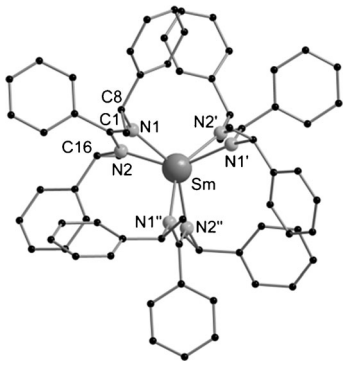

Figure 4. Solid-state structure of compound **8**; hydrogen atoms are omitted for clarity. Selected bond lengths [Å] and angles [°]: Sm–N1 2.440(4), Sm–N2 2.437(4), N1–C1 1.325(6), N1–C8 1.484(6), N2–C1 1.333(6), N2–C16 1.480(5); N1-C1-N2 116.1(4), N1-Sm-N1′ 102.74(11), N1-Sm-N2 55.09(12), N1-Sm-N2′ 110.72(13), C1-N1-C8 118.3(4), C1-N2-C16 119.4(4).

PLATON.[20] A crystallographic *C*3 axis is observed through the hexacoordinated samarium atom. Thus, only a third of the molecule is located in the asymmetric unit. The four-membered metallacycles that are formed by the ligand and the samarium atom (N-C-N-Sm) are slightly rotated with respect to each other, thereby forming a propeller-type structure. Thus, helical chirality, which is typical for trischelate octahedral complexes, is formed. Because the ligands are enantiomerically pure with an all-*S* configuration, in principal, two diastereomers could be formed. In the solid state, we exclusively observed one diastereomer that had the Λ configuration along the helical axis.[19] Thus, the molecule is chiral at the metal center. In contrast to tris-{*N*,*N*′-bis(trimethylsilyl)benzamidinate}samarium(III), which was reported by Edelmann and co-workers,[21] there are no vacant coordination sites at the samarium atom. The center metal atom is completely shielded by the ligands (Figure 5). The Sm–N (Sm–N1 2.440(4) Å, Sm–N2 2.437(4) Å) and N–C1 (N1–C1 1.325(6) Å, N2–C1 1.333(6) Å) distances in complex **8** are comparable to those observed in the mono(amidinate)–samarium complex (**1**). The N1-C1-N2 bite angle (116.1(4)°) is slightly enlarged in comparison to compound **1**.

The ^{1}H NMR spectrum signals of the paramagnetic compound are broadened and shifted compared to those of the (*S*)-KPEBA or bis(amidinate) complexes. There are broad

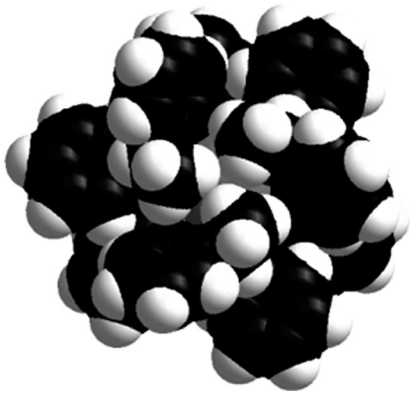

Figure 5. Space-filling representation of the solid-state structure of compound **8**.

singlets for the methyl ($\delta = -2.66$ ppm) and methine groups ($\delta = 3.33$ ppm), both of which are shifted to higher field in comparison to all of the diamagnetic compounds that are discussed herein. Also, the signals for the aromatic protons are broadened and appear in a region between $\delta = 8.98$ and 6.88 ppm. In the $^{13}C\{^1H\}$ NMR spectrum, the methine group also shows one signal ($\delta = 55.4$ ppm), thus indicating that the three ligands bind symmetrically at the samarium center. The signals for the methyl group and the quaternary carbon atom are not observed owing to the paramagnetism of the samarium atom.

We could not isolate the corresponding tris(amidinate)–lutetium complex [{(*S*)-PEBA}$_3$Lu] by amine elimination or salt metathesis. We suggest that the steric strain of the ligands in the potential [{(*S*)-PEBA}$_3$Lu] complex would be too high.

Amido complexes: Based on the knowledge that tris(amidinate) complexes of the smaller rare-earth elements could not be obtained, we developed a straightforward strategy to synthesize chiral amido complexes with the composition [{(*S*)-PEBA}$_2$Ln{N(SiMe$_3$)$_2$}]. These compounds are of special interested because the {N(SiMe$_3$)$_2$}$^-$ group is a potential leaving group in the hydroamination/cyclization catalysis.[22] We have previously communicated that chiral lutetium complex [{(*S*)-PEBA}$_2$Lu{N(SiMe$_3$)$_2$}][15b] can either be obtained by salt metathesis from compound **7** and K{N(SiMe$_3$)$_2$} or by an amine-elimination reaction from (*S*)-HPEBA und [Lu{N(SiMe$_3$)$_2$}$_3$] (Scheme 5).[15b] Because this latter route is more convenient and straightforward, we extended this route to synthesize the corresponding chiral yttrium complex [{(*S*)-PEBA}$_2$Y{N(SiMe$_3$)$_2$}] (**9**).

Compounds **9** and **10** have been investigated by using standard analytic/spectroscopic techniques and their solid-state structures were investigated by single-crystal X-ray diffraction. Because we have previously reported the structure of compound **10**, the structure of compound **9** is only briefly discussed herein. Compound **9** is isostructural to complex **10** and crystallizes in the orthorhombic space group $P2_12_12_1$ with four molecules of the metal complex in the unit cell (Figure 6). The yttrium atom in compound **9** is fivefold coordinated by the nitrogen atoms of the ligands. At first glance, the molecules seems to have a non-crystallographic *C*2 axis along the N5–Y bond but, as already seen in the lutetium complex (**10**), the symmetry is broken by the ligands. Helical chirality (Δ enantiomer[19]) is observed along the pseudo-*C*2 axis. As observed for the previously described enantiopure compounds, only one diastereomer crystallizes. One of the PEBA ligands coordinates in a symmetrical manner to the yttrium atom (Y–N1 2.356(3) Å, Y–N2 2.353(4) Å), whereas the other ligand is slightly asymmetrically coordinated (Y–N3 2.366(4) Å, Y–N4 2.348(3) Å). The Y–N bond lengths in compound **9** (2.266(4)–2.366(4) Å), which are in the expected range,[23] are larger than in compound **10** (2.200(6)–2.305(7) Å), which is a result of the larger ionic radius of the yttrium ion. The {N(SiMe$_3$)$_2$}$^-$ ligand coordinates asymmetrically to the yttrium atom. Thus, the Y–Si2 (3.330(2) Å) distance is smaller than the Y–Si1 distance (3.5157(14) Å), thus resulting in different Y-N-Si bond angles of Y-N5-Si1 (124.3(2)°) and Y-N5-Si2 (112.8(2)°). This deviation is much smaller than expected for an agostic interaction,[24] for ex-

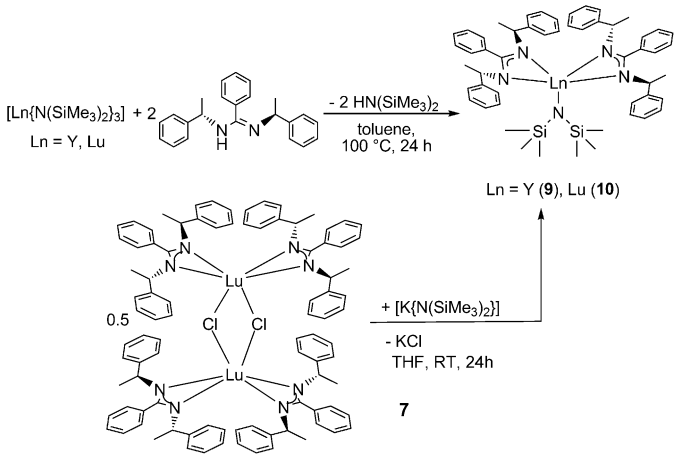

Scheme 5. Synthesis of amido complexes **9** and **10**.

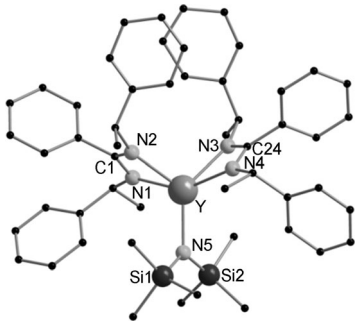

Figure 6. Solid-state structure of compound **9** (compound **10**, which is not shown here, is isostructural); hydrogen atoms are omitted for clarity. Selected bond lengths [Å] and angles [°]: Y–N1 2.356(3), Y–N2 2.353(4), Y–N3 2.366(4), Y–N4 2.348(3), Y–N5 2.266(4), Y–Si1 3.5157(14), Y–Si2 3.330(2), C1–N1 1.341(6), C1–N2 1.333(5), C8–N1 1.464(5), C16–N2 1.476(6), C24–N3 1.343(5), C24–N4 1.345(5), C31–N3 1.480(5), C39–N4 1.469(5), N5–Si1 1.698(4), N5–Si2 1.714(4); N1-Y-N2 57.74(12), N3-Y-N4 57.23(11), N1-C1-N2 116.5(4), N3-C24-N4 114.3(4), Si1-N5-Si2 122.7(2).

ample, in $[(\eta^5\text{-}C_5Me_5)_2Y\{CH(SiMe_3)_2\}]$ (Y-C-Si 138.6(4) and 97.1(3)).[25] Based on these considerations, we suggested packing effects as the reason for the different Y-N-Si angles.

Catalytic hydroamination/cyclization studies: The catalytic hydroamination reaction is the addition of an organic amine N–H bond to a carbon–carbon multiple bond in one step. This straightforward synthetic approach is superior to most of the classical amine syntheses, which consist of multistep reactions and, thus, involve the formation of byproducts and large amounts of chemical waste. Although this reaction is thermodynamically feasible under normal conditions, the high reaction barrier is a significant problem for practical use. Over the last two decades, a large number of hydroamination catalysts that are based on s-, d-, and f-block metal complexes have been developed. The progress in this area over the last decade has been reviewed extensively.[22,26] The enantioselective hydroamination reaction catalyzed by metallocene complexes of the rare-earth elements was pioneered in the 1990s by Marks and co-workers.[27] Nowadays, a number of enantioselective non-metallocene rare-earth-element catalysts are known.[28] Parallel to this development, enantioselective catalysts that are based on other metals have also been reported.[26g,q,29] Nevertheless, there is still a demand for catalysts that can enantioselectively convert a broad range of substrates at moderate temperature with low catalyst loadings.

Complexes **9** and **10** have been investigated as catalysts for the asymmetric intramolecular hydroamination of amino alkenes and for the hydroamination of amino alkynes. These experiments were carried out under rigorously anaerobic conditions in C_6D_6, either at room temperature or at 60 °C, with a catalyst loading of 5 mol %. The conversion was followed by ^{1}H NMR spectroscopy with ferrocene as an internal standard and the *ee* values of the cyclized amino alkenes were determined by ^{19}F NMR spectroscopy of their corresponding Mosher (methoxy(trifluoromethyl)phenylacetyl) amides.[28l,m] In addition, the *ee* values were also measured by chiral HPLC analysis of the corresponding 1-naphthoyl amides, which afforded slightly higher values.[28h] The results are shown in Table 1; for comparison, the values for compound **10** are also shown.

In general, compound **9** showed higher catalytic activity but lower enantioselectivity than compound **10**. This observation is in line with earlier studies, which showed that the rate of the reaction increased with increasing ionic radius of the central metal atom.[30] The suggested turnover-limiting step is the olefin-insertion/cyclization step, which is sterically sensitive.[30–31] Concomitant with the increasing space around the metal center, the stereoselectivity started to decrease. Compounds **9** and **10** showed good activity and all of the substrates were converted regiospecifically into their cyclic products under mild conditions within reasonable reaction times. Although compound **10** is more selective under the same reaction conditions, higher *ee* values could be obtained for substrate **11a** with compound **9** (Table 1, entry 1) because the reaction already proceeded at room temperature. Substrate **12a** (Table 1, entry 2) could also be cyclized into its corresponding spyrocycle at room temperature. In comparison, the lutetium complex (**10**) needed elevated temperatures (60 °C) to catalyze both reactions (Table 1, entries 1 and 2). Amino alkenes **13a** and **14a** did not react at room temperature with compound **9** as the catalyst; instead, a reaction temperature of 60 °C was required.

The differences in the reactivities of substrates **11a**–**13a**, which contained different bulky substituents at the β position to the amino group (Table 1, entries 1–3) can be explained by the Thorpe–Ingold effect.[32]

The *ee* values that were obtained by using compound **10** as the catalyst (**13b**: 75 %, **14b:** 33 %) were significantly higher than those with compound **9** (**13b**: 62 %, **14b:** 13 %). To the best of our knowledge, of all of the previously reported lanthanide-catalyzed asymmetric intramolecular-hydroamination reactions,[26h,j,q] only a very sophisticated thiol-functionalized yttrium complex has shown higher *ee* values for the conversion of substrate **13a**.[28k] This catalyst was

Table 1. Hydroamination of amino alkenes and amino alkynes catalyzed by compounds **9** and **10**.[a]

Entry	Substrate	Product	**9**			**10**		
			t [h]	Yield[d] [%]	*ee*[e] [%]	*t* [h]	Yield[d] [%]	*ee*[e] [%]
1	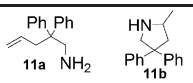 **11a**	**11b**	16[c]	96	66 (*S*)[f]	9[b]	92	61 (*S*)[f]
2	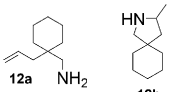 **12a**	**12b**	14[c]	97	66 (*S*)[f]	9[b]	quant	69 (*S*)[f]
3	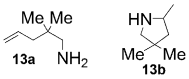 **13a**	**13b**	6.5[b]	quant	62 (*S*)[f]	35[b]	92	75 (*S*)[f]
4	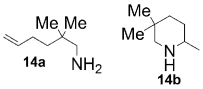 **14a**	**14b**	20[b]	quant	13[g] (*R*)[f]	35[b]	quant	33 (*R*)[f]
5	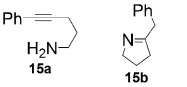 **15a**	**15b**	40[c] 60[b]	45 96	–	108[c]	92	–
6	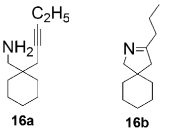 **16a**	**16b**	24[c]	quant	–	85[c]	quant	–

Conditions: [a] Catalyst (15 mg, 5 mol %), C_6D_6; the results for compound **10** are given in reference [15b]. [b] Reaction temperature: 60 °C. [c] Room temperature. [d] Determined by ^{1}H NMR spectroscopy with ferrocene as an internal standard. [e] Enantiomeric excess determined by ^{19}F NMR spectroscopy of Mosher amides. The values determined by chiral HPLC analysis of the 1-naphthoyl amides were slightly higher. [f] Absolute configurations, taken from reference [28l]. [g] Enantiomeric excess determined by chiral HPLC analysis of 1-naphthoyl amides.

only prepared in situ, by treating the protonated ligand with $[Y\{N(SiMe_3)_2\}_3]$, whereas compound **10** is well-characterized and is much more easily accessible.

To evaluate the performance of our catalysts, we also investigated the hydroamination/cyclization reactions of two internal alkynes (Table 1, entries 5 and 6), which formed achiral Schiff bases as products. Quantitative formation of spirocycle **16b** was observed with both catalysts within 24 h (**9**) and 85 h (**10**) at room temperature (Table 1, entry 6). This difference in reactivity between catalysts **9** and **10** was the same as that observed for the other reactions. In contrast, the cyclization of compound **15a** (Table 1, entry 5) stopped after 40 h at a conversion of 45% with catalyst **9**, probably owing to decomposition of the catalyst. To obtain complete cyclization, a reaction temperature of 60°C was necessary.

Conclusion

We have synthesized a series of new chiral lanthanide–amidinate complexes with the PEBA ligand. Whereas mono-, bis-, and tris-substitution of the chloro ligand with the PEBA ligand was possible by using samarium as the metal center, for the smaller lanthanides, lutetium and ytterbium, a homoleptic complex could not be obtained. As a consequence, their bis(amidinate) complexes were readily obtainable in a one-step synthesis. The bis(amidinate) complexes $[\{(S)\text{-PEBA}\}_2Ln\{N(SiMe_3)_2\}]$ (Ln = Y, Lu) were synthesized in one step from their corresponding lanthanide–amides. All of these chiral bis- and tris(amidinate) complexes showed additional axial chirality and they all crystallized as diastereomerically pure compounds. By using *rac*-PEBA as a ligand, an achiral *meso* arrangement of the ligands was observed.

The catalytic activity of $[\{(S)\text{-PEBA}\}_2Ln\{N(SiMe_3)_2\}]$ (Ln = Y, Lu) was investigated in the asymmetric intramolecular hydroamination of amino alkenes and amino alkynes. The yttrium complex showed good activity and all of the substrates tested were converted regiospecifically into their corresponding cyclic products under mild conditions within good reaction times. The catalytic activity was higher and the enantioselectivity was lower than that of the corresponding lutetium complex. The lutetium complex was shown to be a suitable catalyst for the asymmetric intramolecular hydroamination reaction and good enantiomeric excess values were observed for some substrates.

Experimental Section[16]

All of the manipulations of air-sensitive materials were performed with the rigorous exclusion of oxygen and moisture in flame-dried Schlenk-type glassware, either on a dual-manifold Schlenk line that was interfaced to a high-vacuum (10^{-3} mbar) line or in an argon-filled MBraun glove box. THF was distilled under a nitrogen atmosphere from potassium benzophenone ketyl prior to use. Hydrocarbon solvents (toluene and *n*-pentane) were dried by using an Mbraun solvent purification system (SPS-800). All solvents for vacuum-line manipulations were stored in vacuo over $LiAlH_4$ in resealable flasks. Deuterated solvents were obtained from Aldrich GmbH (99 atom% [D]) and were degassed, dried, and stored in vacuo over Na/K alloy in resealable flasks. NMR spectra were recorded on Bruker Avance II 300 MHz or 400 MHz NMR spectrometers. Chemical shifts are referenced to internal solvent and are reported relative to tetramethylsilane. IR spectra were obtained on a Bruker Tensor 37. Mass spectra were recorded at 70 eV on a Finnigan MAT 8200. Elemental analysis was performed on an Elementar vario EL or microcube. $LnCl_3$,[33] $[Ln\{N(SiHMe_2)_2\}_3]$,[34] $[Ln\{N(SiMe_3)_2\}_3]$,[35] (*S*)-HPEBA,[15a] (*S*)-KPEBA,[15a] $[(\{(S)\text{-PEBA}\}_2LuCl)_2]$[15b], and $[\{(S)\text{-PEBA}\}_2Lu\{N(SiMe_3)_2\}]$[15b] were prepared according to literature procedures.

$[(PEBA)LnCl_2(thf)_n]$ (Ln = Sm (1), Yb (2), Lu (3)): THF (10 mL) was condensed at −196°C onto a mixture of $LnCl_3$ (0.71 mmol) and KPEBA (237 mg, 0.65 mmol) and the reaction mixture was stirred overnight at room temperature. The colorless precipitate was filtered off and the solvent was removed in vacuo. The residue was washed with *n*-pentane and the product was crystallized from THF/*n*-pentane.

$[\{(rac)\text{-PEBA}\}SmCl_2(thf)_3]$ (1): Compound **1** was synthesized by the slow addition of a solution of *rac*-KPEBA in THF (5 mL) to a suspension of $SmCl_3$ (183 mg, 0.71 mmol) in THF (10 mL). Yield: 98 mg (0.18 mmol, 28%) as yellow crystals; IR (ATR): $\tilde{\nu}$ = 3056 (w), 3025 (w), 2921 (w), 2874 (w), 1631 (m), 1576 (w), 1490 (m), 1448 (m), 1380 (w), 1347 (w), 1305 (w), 1271 (w), 1207 (w), 1138 (w), 1070 (w), 1027 (w), 913 (w), 878 (w), 761 (m), 698 (s), 624 (w), 604 (w), 572 (w), 542 cm^{-1} (m); elemental analysis calcd (%) for $C_{23}H_{23}N_2Cl_2Sm{\cdot}0.5\,C_4H_8O$: C 51.35, H 4.65, N 4.79; found: C 51.19, H 5.26, N 3.86.

$[\{(S)\text{-PEBA}\}YbCl_2(thf)_2]$ (2): This complex was prepared from $YbCl_3$ (199 mg, 0.71 mmol) and (*S*)-KPEBA. Yield: 134 mg (0.24 mmol, 36%) as orange crystals; IR (ATR): $\tilde{\nu}$ = 3059 (w), 3027 (w), 2970 (w), 2926 (w), 2868 (w), 1625 (m), 1575 (w), 1492 (w), 1448 (w), 1381 (w), 1351 (w), 1308 (w), 1276 (w), 1206 (w), 1134 (w), 1082 (w), 1026 (w), 914 (w),760 (m), 697 (s), 572 (w), 541 cm^{-1} (m); elemental analysis calcd (%) for $C_{23}H_{23}N_2Cl_2Yb{\cdot}2\,C_4H_8O$: C 52.03, H 5.49, N 3.91; found: C 51.22, H 5.40, N 3.68.

$[\{(S)\text{-PEBA}\}LuCl_2(thf)_2]$ (3): This complex was prepared from $LuCl_3$ (200 mg, 0.71 mmol) and (*S*)-KPEBA. Yield: 115 mg (0.16 mmol, 31%) as yellow crystals; ^1H NMR (300 MHz, [D$_8$]THF, 23°C): δ = 7.58–6.76 (m, 15H; Ph), 4.18–4.00 (m, 2H; C*H*), 1.38 ppm (d, ^3J = 6.8 Hz, 6H; CH_3). The complex slowly decomposed in solution and a precipitate was formed; as result no clean NMR spectra could be obtained. IR (ATR): $\tilde{\nu}$ = 3059 (w), 3028 (w), 2956 (w), 2922 (w), 2855 (w), 1633 (m), 1576 (w), 1576 (w), 1488 (w), 1446 (m), 1415 (w), 1353 (w), 1305 (w), 1273 (w), 1209 (w), 1137 (w), 1074 (w), 1024 (w), 912 (w), 798 (w), 761 (m), 697 (s), 542 cm^{-1} (m); elemental analysis calcd (%) for $C_{23}H_{23}N_2Cl_2Lu{\cdot}2\,C_4H_8O$: C 51.89, H 5.48, N 3.90; found: C 51.91, H 5.17, N 3.78.

$[\{(PEBA)_2LnCl\}_2]$ (Ln = Sm (4), Er (5), Yb (6), Lu (7)): THF (10 mL) was condensed at −196°C onto a mixture of $LnCl_3$ (0.55 mmol) and KPEBA (400 mg, 1.09 mmol) and the reaction mixture was stirred overnight at room temperature. The colorless precipitate was filtered off and the solvent was removed in vacuum. The residue was washed with *n*-pentane and the product was crystallized from the specified solvent or solvent mixture.

$[(\{(S)\text{-PEBA}\}_2SmCl)_2]$ (4): Compound **4** was synthesized in two steps. To a suspension of $SmCl_3$ (140 mg, 0.55 mmol) in THF (10 mL) was slowly added a solution of (*S*)-KPEBA (200 mg, 0.55 mmol) in THF (5 mL) and the mixture was stirred overnight at RT. Then, a second portion of (*S*)-KPEBA (200 mg, 0.55 mmol) was dissolved in THF (5 mL), slowly added to the reaction mixture, and stirred for 24 h at room temperature. The product was crystallized from THF/*n*-pentane. Yield: 182 mg (0.22 mmol, 40%) as yellow crystals; ^1H NMR (300 MHz, [D$_8$]THF, 23°C): δ = 7.64–7.61 (m, 1H; Ph), 7.45–7.40 (m, 4H; Ph), 7.35–7.26 (m, 8H; Ph), 7.21–7.12 (m, 5H; Ph), 7.03–6.95 (m, 5H; Ph), 6.90–6.87 (m, 3H; Ph), 5.82–5.79 (m, 2H; Ph), 5.32 (m, 2H; Ph), 4.16 (q, ^3J = 6.5 Hz, 2H; C*H*), 1.50 (d, ^3J = 7.0 Hz, 6H; CH_3), 1.23 ppm (d, ^3J = 6.5 Hz, 6H; CH_3), two protons could not be assigned; $^{13}C\{^1H\}$ NMR (75 MHz, [D$_8$]THF, 23°C): δ = 128.1 (Ph), 127.9 (Ph), 127.8 (Ph), 127.4 (Ph), 126.7 (Ph), 126.1 (Ph), 126.0 (Ph), 157.8 (Ph), 124.9 (Ph), 57.8 (*C*H), 49.9 (*C*H), 26.5 (*C*H$_3$),

22.1 ppm (CH_3), the signals for the quaternary carbon atoms were not observed; IR (ATR): $\tilde{\nu}$ = 3027 (w), 2955 (w), 2920 (w), 1633 (m), 1577 (w), 1487 (m), 1446 (m), 1407 (w), 1349 (w), 1305 (w), 1268 (w), 1208 (w), 1138 (w), 1073 (w), 1025 (w), 910 (w), 760 (m), 697 (s), 600 (w), 572 (w), 541 cm^{-1} (m); MS (EI, 70 eV): *m/z* (%): 826 (4) $[M-Me]^+$, 806 (29) $[M-Cl]^+$, 702 (4), 515 (24), 479 (11), 404 (6), 328 (100) $[PEBA]^+$, 223 (100) $[PEBA-PhEt]^+$, 180 (100), 120 (100) $[PhEtN]^+$, 105 (100) $[PhEt]^+$, 91 (98) $[Bz]^+$, 77 (100) $[Ph]^+$, 57 (49), 42 (80) $[C_2H_4N]^+$, 27 (22) $[CHN]^+$; elemental analysis calcd (%) for $C_{46}H_{46}N_4ClSm$: C 65.72, H 5.52, N 6.66; found: C 65.13, H 5.56, N 6.07.

$[\{(PEBA)_2ErCl\}_2]$ (5): This complex was prepared from $ErCl_3$ (149 mg, 0.55 mmol) and *rac*-KPEBA and crystallized from toluene/*n*-pentane. Yield: 47 mg (0.06 mmol, 10%) as orange crystals; IR (ATR): $\tilde{\nu}$ = 3056 (w), 3026 (w), 2974 (w), 2920 (w), 2875 (w), 1632 (m), 1576 (w), 1486 (m), 1447 (m), 1355 (w), 1303 (w), 1266 (w), 1208 (w), 1138 (w), 1072 (w), 1021 (w), 923 (w), 761 (m), 698 (s), 572 (w), 542 cm^{-1} (m); elemental analysis calcd (%) for $C_{46}H_{46}N_4ClEr{\cdot}C_7H_8$: C 67.03, H 5.73, N 5.90; found: C 67.20, H 5.91, N 5.83.

$[(\{(S)\text{-}PEBA\}_2YbCl)_2]$ (6): This complex was prepared from $YbCl_3$ (152 mg, 0.55 mmol) and (*S*)-KPEBA and crystallized from hot toluene. Yield: 115 mg (0.13 mmol, 24%) as orange crystals; IR (ATR): $\tilde{\nu}$ = 3057 (w), 3025 (w), 2959 (w), 2923 (w), 2871 (w), 1633 (m), 1486 (m), 1445 (m), 1353 (w), 1303 (w), 1269 (w), 1209 (w), 1138 (w), 1072 (w), 1021 (w), 912 (w), 761 (m), 697 (s), 572, 541 cm^{-1} (m); MS (EI, 70 eV): *m/z* (%): 863 (4) $[M]^+$, 848 (20) $[M-Me]^+$, 827 (66) $[M-Cl]^+$, 710 (9), 537 (44), 501 (16), 417 (10), 387 (51), 328 (89) $[PEBA]^+$, 223 (94) $[PEBA-PhEt]^+$, 180 (51), 120 (100) $[PhEtN]^+$, 105 (95) $[PhEt]^+$, 91 (45) $[Bz]^+$, 77 (82) $[Ph]^+$, 51 (18), 42 (30) $[C_2H_4N]^+$, 27 (9) $[CHN]^+$; elemental analysis calcd (%) for $C_{46}H_{46}N_4ClYb{\cdot}C_7H_8$: C 66.62, H 5.70, N 5.86; found: C 66.98, H 5.56, N 5.29.

$[(\{(S)\text{-}PEBA\}_2LuCl)_2]$ (7):[15b] This complex was prepared from $LuCl_3$ (154 mg, 0.55 mmol) and (*S*)-KPEBA and crystallized from toluene/*n*-pentane. Yield: 115 mg (0.13 mmol, 31%) as yellow crystals; ^1H NMR (300 MHz, [D$_8$]THF, 23 °C): δ = 7.47–6.77 (m, 30H; Ph), 4.15 (q, ^3J = 6.6 Hz, 4H; C*H*), 1.44 ppm (d, ^3J = 6.6 Hz, 12H; CH_3); $^{13}C\{^1H\}$ NMR (75 MHz, [D$_8$]THF, 23 °C): δ = 180.3 (N*C*N), 149.3 (*i*-Ph), 136.1 (*i*-Ph), 129.0 (Ph), 128.9 (Ph), 128.8 (Ph), 127.9 (Ph), 126.7 (Ph), 126.2 (Ph), 58.3 (*C*H), 21.7 ppm (*C*H$_3$); IR (ATR): $\tilde{\nu}$ = 3058 (w), 3023 (w), 2963 (m), 2923 (w), 1629 (w), 1488 (w), 1447 (w), 1406 (m), 1366 (m), 1299 (m), 1184 (m), 1154 (w), 1067 (w), 1021 (w), 970 (w), 908 (w), 750 (m), 696 (s), 696 (w), 616 (w), 588 (w), 532 cm^{-1} (w); MS (EI, 70 eV): *m/z* (%): 864 (1) $[M]^+$, 849 (13) $[M-Me]^+$, 829 (57) $[M-Cl]^+$, 759 (16), 703 (9) 537 (9), 501 (7), 417 (6), 328 (68) $[PEBA]^+$, 223 (56) $[PEBA-PhEt]^+$, 180 (18), 120 (100) $[PhEtN]^+$, 105 (100) $[PhEt]^+$, 91 (17) $[Bz]^+$, 77 (42) $[Ph]^+$, 57 (12), 42 (13) $[C_2H_4N]^+$, 27 (4) $[CHN]^+$; elemental analysis calcd (%) for $C_{46}H_{46}N_4ClLu{\cdot}0.5\,C_7H_8$: C 65.23, H 5.53, N 6.15; found: C 65.10, H 5.57, N 5.63.

$[\{(S)\text{-}PEBA\}_3Sm]$ (8): THF (10 mL) was condensed at −196 °C onto a mixture of $[Sm\{N(SiHMe_2)_2\}_3(thf)_2]$ (200 mg, 0.37 mmol) and (*S*)-HPEBA (360 mg, 1.10 mmol). The reaction mixture was stirred overnight at room temperature and the solvent was removed in vacuo. The residue was washed with *n*-pentane and the product was crystallized from hot THF. Yield: 200 mg (0.18 mmol, 48%) as yellow crystals; ^1H NMR (300 MHz, [D$_8$]THF, 23 °C): δ = 8.97 (d, ^3J = 7.1 Hz, 6H; Ph), 8.30 (br s, 9H; Ph), 8.01 (t, ^3J = 7.4 Hz, 6H; Ph), 7.87 (t, ^3J = 7.4 Hz, 3H), 7.49 (br s, 9H; Ph), 7.42–6.88 (m, 12H; Ph), 3.33 (br s, 6H; C*H*), −2.66 ppm (br s, 18H; CH_3); $^{13}C\{^1H\}$ NMR (75 MHz, [D$_8$]THF, 23 °C): δ = 148.4 (*i*-Ph), 139.9 (*i*-Ph), 128.9 (Ph), 128.4 (Ph), 128.4 (Ph), 128.1 (Ph), 127.4 (Ph), 125.8 (Ph), 55.4 ppm (*C*H); IR (ATR): $\tilde{\nu}$ = 3058 (w), 3025 (w), 2956 (w), 2921 (w), 2876 (w), 1635 (m), 1599 (w), 1485 (m), 1447 (m), 1352 (w), 1303 (w), 1265 (w), 1210 (w), 1140 (w), 1070 (w), 1025 (w), 908 (w), 797 (w), 763 (m), 699 (s), 599 (w), 572 (w), 542 cm^{-1} (m); MS (EI, 70 eV): *m/z* (%): 1134 (1) $[M]^+$, 806 (67) $[M-PEBA]^+$, 702 (9), 479 (23), 328 (89) $[PEBA]^+$, 223 (72) $[PEBA-PhEt]^+$, 120 (100) $[PhEtN]^+$, 105 (98) $[PhEt]^+$, 91 (82) $[Bz]^+$, 77 (76) $[Ph]^+$, 41 (19) $[C_2H_3N]^+$, 27 (7) $[CHN]^+$; elemental analysis calcd (%) for $C_{69}H_{69}N_6Sm{\cdot}C_4H_8O$: C 72.77, H 6.44, N 6.98; found: C 72.42, H 6.46, N 6.72.

$[\{(S)\text{-}PEBA\}_2Y\{N(SiMe_3)_2\}]$ (9): Toluene (15 mL) was condensed at −196 °C onto a mixture of $[Y\{N(SiMe_3)_2\}_3]$ (314 mg, 0.55 mmol) and (*S*)-HPEBA (362 mg, 1.1 mmol) and the reaction mixture was stirred overnight at 100 °C. The solvent was removed in vacuum and the product was crystallized from hot *n*-heptane. Yield: 125 mg (0.14 mmol, 25%) as colorless crystals; ^1H NMR (300 MHz, C_6D_6): δ = 7.45–7.00 (m, 30H; Ph), 4.31 (br m, 4H; C*H*), 1.63 (d, ^3J = 6.8 Hz, 12H; CH_3), 0.77 ppm (s, 18H; SiCH_3); $^{13}C\{^1H\}$ NMR (75 MHz, C_6D_6): δ = 179.8 (N*C*N), 148.7 (*i*-Ph), 134.7 (*i*-Ph), 128.2 (Ph), 127.8 (Ph), 127.5 (Ph), 127.1 (Ph), 126.8 (Ph), 126.8 (Ph), 126.1 (Ph), 125.8 (Ph), 58.1 (*C*H), 26.8 (*C*H$_3$), 5.2 ppm (Si*C*H$_3$); $^{29}Si\{^1H\}$ NMR (C_6D_6, 60 MHz): δ = −10.1 ppm; MS (EI, 70 eV): *m/z* (%): 888 (5) $[M-Me]^+$, 743 (74) $[M-\{N(SiMe_3)_2\}]$, 637 (4) $[M-\{N(SiMe_3)_2\}-$PhEt], 576 (31) $[M-PEBA]^+$, 534 (9), 493 (18), 415 (7), 328 (85) $[PEBA]^+$, 313 (15) $[PEBA-Me]^+$, 294 (8), 223 (90) $[PEBA-PhEt]^+$, 209 (22) $[PEBA-PhEt-Me]^+$, 180 (33), 146 (97) $[\{N(SiMe_3)_2\}]^+$, 120 (100) $[PhEtN)^+$, 105 (97) $[PhEt]^+$, 77 (63) $[Ph]^+$, 42 (16) $[C_2H_4N]^+$; IR (ATR): $\tilde{\nu}$ = 3406 (m), 3080 (w), 3059 (w), 3028 (w), 2974 (m), 2955 (m), 2919 (w), 2877 (w), 1636 (s), 1598 (w), 1577 (w), 1559 (w), 1541 (w), 1482 (m), 1450 (m), 1418 (w), 1360 (w), 1347 (w), 1325 (w), 1309 (m), 1267 (w), 1245 (w), 1213 (w), 1180 (w), 1142 (w), 1089 (w), 1072 (m), 1028 (w), 1008 (w), 984 (m), 928 (w), 871 (w), 826 (m), 758 (s), 698 (vs), 666 (m), 602 (m), 572 (m), 544 (s), 466 (w), 419 cm^{-1} (w); elemental analysis calcd (%) for $C_{52}H_{64}N_5Si_2Y$: C 69.07, H 7.13, N 7.75; found: C 69.26, H 7.24, N 7.44.

$[\{(S)\text{-}PEBA\}_2Lu\{N(SiMe_3)_2\}]$ (10):[15b] *Pathway A*. Toluene (10 mL) was condensed onto a mixture of $[Lu\{N(SiMe_3)_2\}_3]$ (572 mg, 0.87 mmol) and (*S*)-HPEBA (573 mg, 1.74 mmol) and the reaction mixture was stirred overnight at 100 °C. After cooling to room temperature, the volatile compounds were removed under vacuum. After washing with *n*-pentane (10 mL), colorless crystals were obtained from a hot solution in *n*-heptane. Yield: 708 mg (0.72 mmol, 82%).

Pathway B. THF (10 mL) was condensed onto a mixture of compound **1** (197 mg, 0.24 mmol) and $KN(SiMe_3)_2$ (45 mg, 0.24 mmol) and the reaction mixture was stirred overnight at room temperature. The colorless precipitate was filtered off and the solvent was removed under vacuum. After washing with of *n*-pentane (10 mL), colorless crystals were obtained from a hot solution in *n*-heptane. Yield: 46 mg (0.05 mmol, 20%); ^1H NMR (300 MHz, C_6D_6, 25 °C): δ = 7.28–6.82 (m, 30H; Ph), 4.29 (br m, 4H; C*H*), 1.53 (d, ^3J = 6.8 Hz, 12H; CH_3), 0.66 ppm (s, 18H; SiCH_3); $^{13}C\{^1H\}$ NMR (75 MHz, C_6D_6, 25 °C): δ = 179.4 (N*C*N), 148.6 (*i*-Ph), 134.9 (*i*-Ph), 127.9 (Ph), 127.1 (Ph), 126.9 (Ph), 126.4 (Ph), 126.2 (Ph), 126.0 (Ph), 57.6 (*C*H), 27.1 (*C*H$_3$), 5.5 ppm (Si*C*H$_3$); $^{29}Si\{^1H\}$ NMR (60 MHz, C_6D_6, 25 °C): δ = −9.3 ppm; MS (EI, 70 eV): *m/z* (%): 989 (1) $[M]^+$, 974 (34) $[M-Me]^+$, 854 (11), 828 (16) $[M-\{N(SiMe_3)_2\}]^+$, 723 (21) $[M-\{N(SiMe_3)_2\}-PhEt]^+$, 662 (63) $[M-PEBA]^+$, 579 (31), 480 (17), 380 (23), 328 (87) $[PEBA]^+$, 223 (68) $[PEBA-PhEt]^+$, 180 (77), 146 (98) $[N(SiMe_3)_2]^+$, 120 (96) $[PhEtN]^+$, 105 (100) $[PhEt]^+$, 91 (74) $[Bz]^+$, 77 (90) $[Ph]^+$, 42 (100) $[C_2H_4N]^+$; IR (ATR): $\tilde{\nu}$ = 3057 (w), 3023 (w), 2973 (w), 2954 (w), 2919 (w), 2919 (w), 2877 (w), 2857 (w), 1636 (m), 1598 (w), 1578 (w), 1483 (m), 1448 (m), 1360 (w), 1306 (w), 1266 (w), 1212 (w), 1142 (w), 1072 (w), 1027 (w), 1006 (w), 969 (w), 929 (w), 829 (w), 762 (m), 698 (s), 601 (w), 572 (w), 544 cm^{-1} (m); elemental analysis calcd (%) for $C_{52}H_{64}N_5Si_2Lu{\cdot}1.5\,C_7H_8$: C 66.52, H 6.79, N 6.21; found: C 66.61, H 6.46, N 6.25.

Hydroamination reactions: The catalyst was weighed into a NMR tube under an argon atmosphere. C_6D_6 (about 0.5 mL) was condensed into the NMR tube and the mixture was frozen at −196 °C. The reactant was injected onto the solid mixture and the whole sample was melted and mixed just before insertion into the core of the NMR machine (t_0). The ratio between the reactant and the product was calculated by comparison of the integrations of the corresponding signals. Ferrocene was used as an internal standard for the kinetic measurements. The substrates 2,2-diphenyl-pent-4-enylamine (**11a**),[28m] C-(1-allyl-cyclohexyl)-methylamine (**12a**),[28m] 2,2-dimethylpent-4-en-1-amine (**13a**),[28m] 2,2-dimethylhex-5-en-1-amine (**14a**),[28l] 5-phenylpent-4-yn-1-amine (**15a**),[37] and [1-(pent-2-ynyl)-cyclohexyl]methanamine (**16a**)[31] were synthesized according to literature procedures. The ^1H NMR data of 2-methyl-4,4-diphenylpyrroli-

dine (**11b**),[28m] 3-methyl-2-aza-spiro-[4.5]decane (**12b**),[28m] 2,4,4-trimethylpyrrolidine (**13b**),[28m] 2,5,5-trimethylpiperidine (**14b**),[37] 2-benzyl-1-pyrroline (**15b**),[36] and 3-propyl-2-azaspiro[4.5]dec-2-ene (**16b**)[31] conformed with literature data.

General procedure for the preparation of Mosher amides: The cyclic amine (0.1–0.2 mmol) was dissolved in dry $CDCl_3$ (0.5 mL) in an NMR tube. Then, Et_3N (2 equiv) and (*S*)-(+)-α-methoxy-α-trifluoromethylphenylacetic acid chloride (2–5 equiv) were added. Afterwards, the enantiomeric excess was determined by ^{19}F NMR spectroscopy at 60–70 °C.[28l]

Mosher adduct of: **11b**: ^{19}F NMR ($CDCl_3$, 70 °C): $\delta = -69.3$ (major isomer), −70.4 ppm (minor isomer); **12b**: ^{19}F NMR ($CDCl_3$, 70 °C): $\delta = -69.7$ (major isomer), −70.6 ppm (minor isomer); **13b**: ^{19}F NMR ($CDCl_3$, 60 °C): $\delta = -69.7$ (major isomer), −70.6 ppm (minor isomer); The ^{19}F NMR spectra are provided in the Supporting Information.

The ^{19}F NMR spectrum of the Mosher adduct of compound **14b** showed an indefinable mixture of products and the enantiomeric excess of compound **14b** was determined by chiral HPLC analysis of the corresponding 1-naphthoyl amide.

Determination of enantiomeric excess by chiral HPLC analysis: The hydroamination products were derivatized as 1-naphthoyl amides by treating with 1-naphthoyl chloride (1 equiv) and Et_3N (3 equiv) in CH_2Cl_2.[28h] The *ee* values of the products were determined by HPLC analysis on a chiral stationary phase (Regis (*R*,*R*)-β-Gem1 column, i.d.: 4.6 mm, length: 250 mm, particle size: 5 mm). The HPLC conditions and *ee* values are shown in Table 1.

X-ray crystallographic studies of compounds 1–10: Suitable crystals of compounds **1**–**10** were covered in mineral oil (Aldrich) and mounted onto a glass fiber. The crystals were transferred directly into the cold stream of a Stoe IPDS 2 or Stoe IPDS 2T diffractometer (−73 °C or −123 °C N_2). Data were corrected for absorption effects by using indexed faces of the crystals.[38]

All structures were solved by using the program SHELXS-97.[39] The remaining non-hydrogen atoms were located from successive difference Fourier map calculations. The refinements were carried out by using full-matrix least-squares techniques on F^2, by minimizing the function $(F_o - F_c)^2$, where the weight was defined as $4F_o^2/2(F_o^2)$ and F_o and F_c were the observed- and calculated structure factor amplitudes, respectively, by using the program SHELXL-97.[39] The hydrogen atom contributions of all of the compounds were calculated, but not refined. In each case, the locations of the largest peaks in the final difference Fourier map calculations, as well as the magnitude of the residual electron densities, were of no chemical significance. The structures of compound **7** and **10** have been reported previously.[15b]

Crystal data for compound **1**: $C_{35}H_{47}Cl_2N_2O_3Sm$; $M_w = 765.00$; monoclinic; $a = 13.440(3)$, $b = 11.421(2)$, $c = 24.267(8)$ Å; $\beta = 108.69(3)°$; $V = 3528.5(17)$ Å^3; $T = 200(2)$ K; space group $P2_1/c$; $Z = 4$; total reflns 105130; unique reflns 7465 ($R_{int} = 0.0573$); final R_1 values were 0.0270 ($I > 2\sigma(I)$); final $wR(F^2)$ values were 0.0696 (all data); GOF on F^2 was 1.088; Flack parameter = −0.025(11).

Crystal data for compound **2**: $C_{31}H_{39}Cl_2N_2O_2Yb$; $M_w = 715.58$; monoclinic; $a = 13.242(3)$, $b = 12.530(3)$, $c = 10.896(2)$ Å; $\beta = 118.64(3)°$; $V = 1586.7(8)$ Å^3; $T = 200(2)$ K; space group $C2$; $Z = 2$; total reflns 27046; unique reflns 4253 ($R_{int} = 0.1049$); final R_1 values were 0.0281 (($I > 2\sigma(I)$); final $wR(F^2)$ values were 0.0723 (all data); GOF on F^2 was 1.045; Flack parameter = −0.025(11).

Crystal data for compound **3**: $C_{31}H_{39}Cl_2LuN_2O_2$; $M_w = 717.51$; monoclinic; $a = 13.1521(11)$, $b = 12.4744(11)$, $c = 10.8067(9)$ Å; $\beta = 118.413(6)°$; $V = 1559.4(2)$ Å^3; $T = 150(2)$ K; space group $C2$; $Z = 2$; total reflns 6017; unique reflns 3278 ($R_{int} = 0.0330$); final R_1 values were 0.0193 ($I > 2\sigma(I)$); final $wR(F^2)$ values were 0.0488 (all data); GOF on F^2 was 1.039; Flack parameter = −0.014(8).

Crystal data for compound **4**: $C_{92}H_{92}Cl_2N_8Sm_2$; $M_w = 1681.34$; cubic; $a = 24.754(3)$ Å; $V = 15169(3)$ Å^3; $T = 150(2)$ K; space group $I23$; $Z = 6$; total reflns 66110; unique reflns 6068 ($R_{int} = 0.0567$); final R_1 values were 0.0352 ($I > 2\sigma(I)$); final $wR(F^2)$ values were 0.1069 (all data); GOF on F^2 was 1.229; Flack parameter = 0.020(16).

Crystal data for compound **5**: "$2(C_{92}H_{92}Cl_2Er_2N_8)\cdot C_5H_{12}$"; $M_w = 3502.46$; triclinic; $a = 14.149(3)$, $b = 16.590(3)$, $c = 19.387(4)$ Å; $\alpha = 86.88(3)$, $\beta = 84.03(3)$, $\gamma = 71.25(3)°$; $V = 4284.8(15)$ Å^3; $T = 200(2)$ K; space group $P\bar{1}$; $Z = 1$; total reflns 119819; unique reflns 23140 ($R_{int} = 0.1724$); final R_1 values were 0.0689 ($I > 2\sigma(I)$); final $wR(F^2)$ values were 0.1287 (all data); GOF on F^2 was 1.104; Flack parameter = 0.008(11).

Crystal data for compound **6**: $C_{92}H_{92}Cl_2N_8Yb_2$; $M_w = 1726.72$; cubic; $a = 24.596(3)$ Å; $V = 14880(3)$ Å^3; $T = 200(2)$ K; space group $I23$; $Z = 6$; total reflns 10393; unique reflns 4574 ($R_{int} = 0.0419$); final R_1 values were 0.0263 ($I > 2\sigma(I)$); final $wR(F^2)$ values were 0.0676 (all data); GOF on F^2 was 1.049; Flack parameter = −0.006(9).

Crystal data for compound **8**: $C_{69}H_{69}N_6Sm$; $M_w = 1132.65$; cubic; $a = 18.5719(6)$ Å; $V = 6405.7(4)$ Å^3; $T = 200(2)$ K; space group $P2_13$; $Z = 4$; total reflns 33649; unique reflns 3873 ($R_{int} = 0.0641$); final R_1 values were 0.0349 ($I > 2\sigma(I)$); final $wR(F^2)$ values were 0.0868 (all data); GOF on F^2 was 1.035; Flack parameter = −0.021(6).

Crystal data for compound **9**: $C_{52}H_{64}N_5Si_2Y$; $M_w = 904.17$; orthorhombic; $a = 10.148(2)$, $b = 10.675(2)$, $c = 45.563(9)$ Å; $V = 4935.7(17)$ Å^3; $T = 150(2)$ K; space group $P2_12_12_1$; $Z = 4$; total reflns 39095; unique reflns 8243 ($R_{int} = 0.1222$); final R_1 values were 0.0455 ($I > 2\sigma(I)$); final $wR(F^2)$ values were 0.0893 (all data); GOF on F^2 was 0.912; Flack parameter = −0.021(6).

CCDC-884826 (**1**), CCDC-884827 (**2**), CCDC-884828 (**3**), CCDC-884829 (**4**), CCDC-884830 (**5**), CCDC-884831 (**8**), and CCDC-884832 (**9**) contain the supplementary crystallographic data for this paper. These data can be obtained free of charge from The Cambridge Crystallographic Data Centre via www.ccdc.cam.ac.uk/data_request/cif.

Acknowledgements

J.K. thanks the Landesgraduiertenförderung for support.

[1] a) A. A. Trifonov, *Coord. Chem. Rev.* **2010**, *254*, 1327–1347; b) F. T. Edelmann, F. H. Anthony, J. F. Mark in *Chapter 3 Advances in the Coordination Chemistry of Amidinate and Guanidinate Ligands, Vol. 57* Academic Press, **2008**, pp. 183–352; c) P. C. Junk, M. L. Cole, *Chem. Commun.* **2007**, 1579–1590.

[2] a) M. Wedler, F. Knösel, U. Pieper, D. Stalke, F. T. Edelmann, H.-D. Amberger, *Chem. Ber.* **1992**, *125*, 2171–2181; b) F. T. Edelmann, *Chem. Soc. Rev.* **2009**, *38*, 2253–2268.

[3] a) F. T. Edelmann, *Top. Curr. Chem.* **1996**, *179*, 113–148; b) F. T. Edelmann, *Struct. Bonding (Berlin)* **2010**, *137*, 109–164; c) F. T. Edelmann, *Angew. Chem.* **1995**, *107*, 2647–2669; *Angew. Chem. Int. Ed. Engl.* **1995**, *34*, 2466–2488.

[4] a) F. T. Edelmann, *J. Alloys Compd.* **1994**, *207–208*, 182–188; b) J. R. Hagadorn, J. Arnold, *Organometallics* **1996**, *15*, 984–991.

[5] S. Bambirra, D. van Leusen, A. Meetsma, B. Hessen, J. H. Teuben, *Chem. Commun.* **2003**, 522–523.

[6] a) L. Zhang, M. Nishiura, M. Yuki, Y. Luo, Z. Hou, *Angew. Chem.* **2008**, *120*, 2682–2685; b) V. Y. Rad′kov, G. G. Skvortsov, D. M. Lyubov, A. V. Cherkasov, G. K. Fukin, A. S. Shavyrin, D. Cui, A. A. Trifonov, *Eur. J. Inorg. Chem.* **2012**, 2289–2297; c) S. Bambirra, M. W. Bouwkamp, A. Meetsma, B. Hessen, *J. Am. Chem. Soc.* **2004**, *126*, 9182–9183.

[7] E. A. Bijpost, R. Duchateau, J. H. Teuben, *J. Mol. Catal. A* **1995**, *95*, 121–128.

[8] S. Ge, A. Meetsma, B. Hessen, *Organometallics* **2008**, *27*, 3131–3135.

[9] S. Bambirra, H. Tsurugi, D. van Leusen, B. Hessen, *Dalton Trans.* **2006**, 1157–1161.

[10] a) Y. Luo, Y. Yao, Q. Shen, J. Sun, L. Weng, *J. Organomet. Chem.* **2002**, *662*, 144–149; b) A. A. Trifonov in *Rare-Earth Metal Complexes Supported by Nitrogen-Containing Ligands in Olefin Polymerization Olefin Upgrading Catalysis by Nitrogen-based Metal Com-*

plexes I, Vol. 35 (Eds.: J. Campora, G. Giambastiani), Springer, Netherlands, **2011**, pp. 119–152.
[11] a) C. Averbuj, E. Tish, M. S. Eisen, *J. Am. Chem. Soc.* **1998**, *120*, 8640–8646; b) J. Li, S. Huang, L. Weng, D. Liu, *J. Organomet. Chem.* **2006**, *691*, 3003–3010; c) L. A. Koterwas, J. C. Fettinger, L. R. Sita, *Organometallics* **1999**, *18*, 4183–4190.
[12] H. Brunner, J. Lukassek, G. Agrifoglio, *J. Organomet. Chem.* **1980**, *195*, 63–76.
[13] E. Nelkenbaum, M. Kapon, M. S. Eisen, *J. Organomet. Chem.* **2005**, *690*, 3154–3164.
[14] a) A. Bertogg, A. Togni, *Organometallics* **2006**, *25*, 622–630; b) H. Brunner, G. Agrifoglio, *Monatsh. Chem.* **1980**, *111*, 275–287.
[15] a) P. Benndorf, C. Preuß, P. W. Roesky, *J. Organomet. Chem.* **2011**, *696*, 1150–1155; b) P. Benndorf, J. Jenter, L. Zielke, P. W. Roesky, *Chem. Commun.* **2011**, *47*, 2574–2576.
[16] P. Benndorf, *Dissertation*, Karlsruher Institut für Technologie (KIT), Karlsruhe, **2010**.
[17] R. Shannon, *Acta Crystallographica Section A* **1976**, *32*, 751–767.
[18] A. Trifonov, G. Skvortsov, D. Lyubov, G. Fukin, E. Fedorova, M. Bochkarev, *Russ. Chem. Bull.* **2005**, *54*, 2511–2518.
[19] F. A. Cotton, G. Wilkinson, *Advanced Inorganic Chemistry*, Wiley-Interscience, New York, **1988**, p. 54.
[20] A. L. Spek, *J. Appl. Crystallogr.* **2003**, *36*, 7–13.
[21] J. Richter, J. Feiling, H.-G. Schmidt, M. Noltemeyer, W. Brüser, F. T. Edelmann, *Z. Anorg. Allgem. Chem.* **2004**, *630*, 1269–1275.
[22] S. Hong, T. J. Marks, *Acc. Chem. Res.* **2004**, *37*, 673–686.
[23] a) J. A. R. Schmidt, J. Arnold, *Chem. Commun.* **1999**, 2149–2150; b) Y. Luo, P. Xu, Y. Lei, Y. Zhang, Y. Wang, *Inorg. Chim. Acta* **2010**, *363*, 3597–3601.
[24] W. Scherer, D. J. Wolstenholme, V. Herz, G. Eickerling, A. Brück, P. Benndorf, P. W. Roesky, *Angew. Chem.* **2010**, *122*, 2291–2295; *Angew. Chem. Int. Ed.* **2010**, *49*, 2242–2246.
[25] K. H. Den Haan, J. L. De Boer, J. H. Teuben, A. L. Spek, B. Kojic-Prodic, G. R. Hays, R. Huis, *Organometallics* **1986**, *5*, 1726–1733.
[26] a) J. Seayad, A. Tillack, C. G. Hartung, M. Beller, *Adv. Synth. Catal.* **2002**, *344*, 795–813; b) I. Bytschkov, S. Doye, *Eur. J. Org. Chem.* **2003**, 935–946; c) F. Pohlki, S. Doye, *Chem. Soc. Rev.* **2003**, *32*, 104–114; d) P. W. Roesky, T. E. Müller, *Angew. Chem.* **2003**, *115*, 2812–2814; *Angew. Chem. Int. Ed.* **2003**, *42*, 2708–2710; e) F. Alonso, I. P. Beletskaya, M. Yus, *Chem. Rev.* **2004**, *104*, 3079–3160; f) J. F. Hartwig, *Pure Appl. Chem.* **2004**, *76*, 507–516; g) K. C. Hultzsch, *Adv. Synth. Catal.* **2005**, *347*, 367–391; h) K. C. Hultzsch, *Org. Biomol. Chem.* **2005**, *3*, 1819–1824; i) R. A. Widenhoefer, X. Han, *Eur. J. Org. Chem.* **2006**, 4555–4563; j) I. Aillaud, J. Collin, J. Hannedouche, E. Schulz, *Dalton Trans.* **2007**, 5105–5118; k) J.-J. Brunet, N.-C. Chu, M. Rodriguez-Zubiri, *Eur. J. Inorg. Chem.* **2007**, 4711–4722; l) P. A. Hunt, *Dalton Trans.* **2007**, 1743–1754; m) A. V. Lee, L. L. Schafer, *Eur. J. Inorg. Chem.* **2007**, 2245–2255; n) R. Severin, S. Doye, *Chem. Soc. Rev.* **2007**, *36*, 1407–1420; o) E. Smolensky, M. S. Eisen, *Dalton Trans.* **2007**, 5623–5650; p) T. Andrea, M. S. Eisen, *Chem. Soc. Rev.* **2008**, *37*, 550–567; q) T. E. Müller, K. C. Hultzsch, M. Yus, F. Foubelo, M. Tada, *Chem. Rev.* **2008**, *108*, 3795–3892; r) R. Dorta in *Iridium-Catalyzed Hydroamination*, Wiley-VCH, Weinheim, **2009**, pp. 145–172; s) P. W. Roesky, *Angew. Chem.* **2009**, *121*, 4988–4991; *Angew. Chem. Int. Ed.* **2009**, *48*, 4892–4894; t) G. Zi, *Dalton Trans.* **2009**, 9101–9109; u) K. D. Hesp, M. Stradiotto, *ChemCatChem* **2010**, *2*, 1192–1207; v) T. Li, J. Jenter, P. W. Roesky, *Struct. Bonding (Berlin)* **2010**, *137*, 165–228; w) A. L. Reznichenko, K. C. Hultzsch in *Asymmetric Hydroamination*, Wiley-VCH, Weinheim, **2010**, pp. 341–375; x) J. G. Taylor, L. A. Adrio, K. K. Hii, *Dalton Trans.* **2010**, *39*, 1171–1175; y) B. Alcaide, P. Almendros, *Adv. Synth. Catal.* **2011**, *353*, 2561–2576; z) E. M. Beccalli, G. Broggini, A. Fasana, M. Rigamonti, *J. Organomet. Chem.* **2011**, *696*, 277–295; aa) D. Crozet, M. Urrutigoïty, P. Kalck, *ChemCatChem* **2011**, *3*, 1102–1118; ab) G.-F. Zi, *J. Organomet. Chem.* **2011**, *696*, 68–75; ac) J. Jenter, A. Lühl, P. W. Roesky, S. Blechert, *J. Organomet. Chem.* **2011**, *696*, 406–418; ad) X.-Y. Liu, Z. Guo, S. S. Dong, X.-H. Li, C.-M. Che, *Chem. Eur. J.* **2011**, *17*, 12932–12945.
[27] a) M. A. Giardello, V. P. Conticello, L. Brard, M. R. Gagne, T. J. Marks, *J. Am. Chem. Soc.* **1994**, *116*, 10241–10254; b) M. R. Gagne, L. Brard, V. P. Conticello, M. A. Giardello, C. L. Stern, T. J. Marks, *Organometallics* **1992**, *11*, 2003–2005; c) S. Hong, A. M. Kawaoka, T. J. Marks, *J. Am. Chem. Soc.* **2003**, *125*, 15878–15892.
[28] a) I. Aillaud, C. Olier, Y. Chapurina, J. Collin, E. Schulz, R. g. Guillot, J. r. m. Hannedouche, A. Trifonov, *Organometallics* **2011**, *30*, 3378–3385; b) J. Collin, J.-C. Daran, E. Schulz, A. Trifonov, *Chem. Commun.* **2003**, 3048–3049; c) D. V. Gribkov, K. C. Hultzsch, F. Hampel, *Chem. Eur. J.* **2003**, *9*, 4796–4810; d) P. N. O′Shaughnessy, P. D. Knight, C. Morton, K. M. Gillespie, P. Scott, *Chem. Commun.* **2003**, 1770–1771; e) P. N. O′Shaughnessy, P. Scott, *Tetrahedron: Asymmetry* **2003**, *14*, 1979–1983; f) Y. K. Kim, T. Livinghouse, Y. Horino, *J. Am. Chem. Soc.* **2003**, *125*, 9560–9561; g) D. V. Gribkov, K. C. Hultzsch, *Chem. Commun.* **2004**, 730–731; h) S. Hong, S. Tian, M. V. Metz, T. J. Marks, *J. Am. Chem. Soc.* **2003**, *125*, 14768–14783; i) I. Aillaud, D. Lyubov, J. Collin, R. Guillot, J. Hannedouche, E. Schulz, A. Trifonov, *Organometallics* **2008**, *27*, 5929–5936; j) I. Aillaud, J. Collin, C. Duhayon, R. Guillot, D. Lyubov, E. Schulz, A. Trifonov, *Chem. Eur. J.* **2008**, *14*, 2189–2200; k) J. Y. Kim, T. Livinghouse, *Org. Lett.* **2005**, *7*, 1737–1739; l) D. V. Gribkov, K. C. Hultzsch, F. Hampel, *J. Am. Chem. Soc.* **2006**, *128*, 3748–3759; m) P. H. Martinez, K. C. Hultzsch, F. Hampel, *Chem. Commun.* **2006**, 2221–2223; n) A. L. Reznichenko, H. N. Nguyen, K. C. Hultzsch, *Angew. Chem.* **2010**, *122*, 9168–9171; *Angew. Chem. Int. Ed.* **2010**, *49*, 8984–8987; o) N. Meyer, A. Zulys, P. W. Roesky, *Organometallics* **2006**, *25*, 4179–4182.
[29] a) A. L. Gott, A. J. Clarke, G. J. Clarkson, P. Scott, *Organometallics* **2007**, *26*, 1729–1737; b) M. C. Wood, D. C. Leitch, C. S. Yeung, J. A. Kozak, L. L. Schafer, *Angew. Chem.* **2006**, *119*, 358–362; *Angew. Chem. Int. Ed.* **2006**, *46*, 354–358; c) T. Ogata, A. Ujihara, S. Tsuchida, T. Shimizu, A. Kaneshige, K. Tomioka, *Tetrahedron Lett.* **2007**, *48*, 6648–6650; d) X. Shen, S. L. Buchwald, *Angew. Chem.* **2010**, *122*, 574–577; *Angew. Chem. Int. Ed.* **2010**, *49*, 564–567; e) K. Manna, S. Xu, A. D. Sadow, *Angew. Chem.* **2011**, *123*, 1905–1908; *Angew. Chem. Int. Ed.* **2011**, *50*, 1865–1868; f) X. Zhang, T. J. Emge, K. C. Hultzsch, *Angew. Chem. Int. Ed.* **2012**, *51*, 394–398.
[30] M. R. Gagne, C. L. Stern, T. J. Marks, *J. Am. Chem. Soc.* **1992**, *114*, 275–294.
[31] M. Rastätter, A. Zulys, P. W. Roesky, *Chem. Eur. J.* **2007**, *13*, 3606–3616.
[32] M. E. Jung, G. Piizzi, *Chem. Rev.* **2005**, *105*, 1735–1766.
[33] M. D. Taylor, C. P. Carter, *J. Inorg. Nucl. Chem.* **1962**, *24*, 387–391.
[34] R. Anwander, O. Runte, J. Eppinger, G. Gerstberger, E. Herdtweck, M. Spiegler, *J. Chem. Soc. Dalton Trans.* **1998**, 847–858.
[35] D. C. Bradley, J. S. Ghotra, F. A. Hart, *J. Chem. Soc. Dalton Trans.* **1973**, 1021–1023.
[36] Y. Li, T. J. Marks, *J. Am. Chem. Soc.* **1996**, *118*, 9295–9306.
[37] M. R. Crimmin, M. Arrowsmith, A. G. M. Barrett, I. J. Casely, M. S. Hill, P. A. Procopiou, *J. Am. Chem. Soc.* **2009**, *131*, 9670–9685.
[38] Stoe&Cie in *X-AREA and X-RED32*, Darmstadt, Germany, **2006**.
[39] G. M. Sheldrick, *Acta Crystallogr. Sect. A* **2008**, *64*, 112–122.

Received: July 10, 2012
Published online: ■■ ■■, 0000

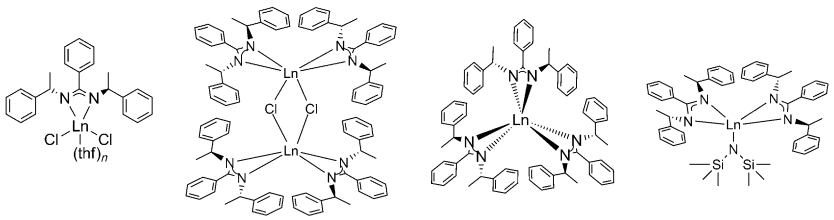

Enantiomerically pure lanthanide complexes were synthesized as the first rare-earth-metal complexes containing a chiral amidinate ligand. The catalytic activities and enantioselectivities of these complexes were studied in hydroamination reactions.

Lanthanide Complexes

*P. Benndorf, J. Kratsch, L. Hartenstein, C. M. Preuss, P. W. Roesky** ■■■■–■■■■

Chiral Benzamidinate Ligands in Rare-Earth-Metal Coordination Chemistry